

As concrete example we go back over again to the AIM: We start by explicitly setting up Eq. (6.67) for the fourth-order kernels entering the GME for the populations. Thereby we notice that the allowed change in the particle number is also determined by the subgroup index

$$\begin{aligned}
 G.(0) & \longleftrightarrow \Delta N = 0 \\
 G.(1) & \longleftrightarrow \Delta N = \pm 1 \\
 G.(2) & \longleftrightarrow \Delta N = 0, \pm 2
 \end{aligned} \tag{4.74}$$

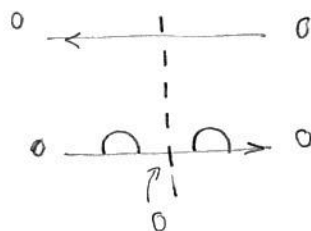
Hence, we identify in fourth order the following non zero contributions:

(the notes are in 4th order but we omit for simplicity the index (4))

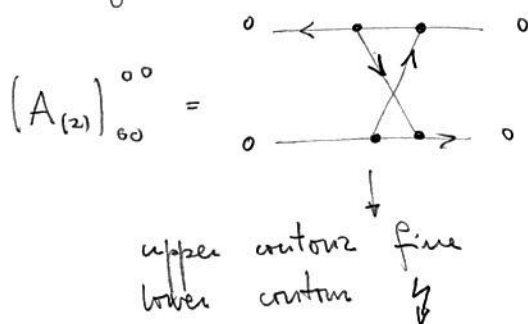
$$(K^{(4)})_{00}^{00} = - \left(\sum_{\sigma} \Gamma^{0 \rightarrow \sigma} + \Gamma^{0 \rightarrow 2} \right) = (A_{(01)})_{00}^{00} + (C_{(01)})_{00}^{00} + (B_{(2)})_{00}^{00} + (C_{(2)})_{00}^{00} \tag{4.75a}$$

Notice that $(B_{(01)})_{00}^{00}$ and $(A_{(2)})_{00}^{00}$ have been omitted. The reason is different for the α graphs:

$(B_{(01)})_{00}^{00}$ has, for the AIM only scalar contributions in the free evolution component.



\Rightarrow is absent from the kernel



Independent of the precise form of the crossing, fermionic lines cannot be assigned consistently since $d_{\sigma} |0\rangle = 0$.

Analogously:

$$(K^{(4)})_{00}^{\bar{\sigma}\bar{\sigma}} = \Gamma^{\bar{\sigma} \rightarrow 0} = (A_{(1)})_{00}^{\bar{\sigma}\bar{\sigma}} + (B_{(1)})_{00}^{\bar{\sigma}\bar{\sigma}} + (C_{(1)})_{00}^{\bar{\sigma}\bar{\sigma}} \quad (4.75b)$$

$$(K^{(4)})_{00}^{22} = \Gamma^{2 \rightarrow 0} = (A_{(2)})_{00}^{22} + (C_{(2)})_{00}^{22}$$

where we have excluded the $(B_{(2)})_{00}^{22}$ since in $B_{(2)}$ the fermionic lines start and end on the same contour $\Rightarrow \Delta N = 0$.

We continue with the other elements of the 4th order kernel

$$\begin{aligned} (K^{(4)})_{\bar{\sigma}\bar{\sigma}}^{\bar{\sigma}\bar{\sigma}} &= - \left(\Gamma^{\bar{\sigma} \rightarrow 0} + \Gamma^{\bar{\sigma} \rightarrow \bar{\sigma}} + \Gamma^{\bar{\sigma} \rightarrow 2} \right) \\ &= (A_{(1)})_{\bar{\sigma}\bar{\sigma}}^{\bar{\sigma}\bar{\sigma}} + (C_{(1)})_{\bar{\sigma}\bar{\sigma}}^{\bar{\sigma}\bar{\sigma}} + (A_{(2)})_{\bar{\sigma}\bar{\sigma}}^{\bar{\sigma}\bar{\sigma}} + (B_{(2)})_{\bar{\sigma}\bar{\sigma}}^{\bar{\sigma}\bar{\sigma}} + (C_{(2)})_{\bar{\sigma}\bar{\sigma}}^{\bar{\sigma}\bar{\sigma}} \end{aligned} \quad (4.76a)$$

$$(K^{(4)})_{\bar{\sigma}\bar{\sigma}}^{\bar{\sigma}\bar{\sigma}} = \Gamma^{\bar{\sigma} \rightarrow \bar{\sigma}} = (A_{(2)})_{\bar{\sigma}\bar{\sigma}}^{\bar{\sigma}\bar{\sigma}} + (C_{(2)})_{\bar{\sigma}\bar{\sigma}}^{\bar{\sigma}\bar{\sigma}}$$

Here the $G_{(1)}$ groups are excluded since their structure with the 4 vertices on the same contour imply the same initial and final state. Moreover, the group $B_{(2)}$ is excluded, for the same reason (2 vertices per contour closed in pair on the same contour).

We continue with the 2 regular cases

$$(K^{(4)})_{\bar{\sigma}\bar{\sigma}}^{00} = \Gamma^{0 \rightarrow \bar{\sigma}} = (A_{(1)})_{\bar{\sigma}\bar{\sigma}}^{00} + (B_{(1)})_{\bar{\sigma}\bar{\sigma}}^{00} + (C_{(1)})_{\bar{\sigma}\bar{\sigma}}^{00} \quad (4.76b)$$

$$(K^{(4)})_{\bar{\sigma}\bar{\sigma}}^{22} = \Gamma^{2 \rightarrow \bar{\sigma}} = (A_{(1)})_{\bar{\sigma}\bar{\sigma}}^{22} + (B_{(1)})_{\bar{\sigma}\bar{\sigma}}^{22} + (C_{(1)})_{\bar{\sigma}\bar{\sigma}}^{22}$$

Finally for the transitions from/to the 2 particle state

$$(K^{(4)})_{22}^{22} = - \left(\sum_{\bar{\sigma}} \Gamma^{2 \rightarrow \bar{\sigma}} + \Gamma^{2 \rightarrow 0} \right) = (A_{(1)})_{22}^{22} + (C_{(1)})_{22}^{22} + (B_{(2)})_{22}^{22} + (C_{(2)})_{22}^{22}$$

Here the situation is symmetrical to the one obtained for $(4.77a)$

the diagrams carrying the co-st effects are $A_{(1|1)}$, $C_{(1|1)}$ respectively.

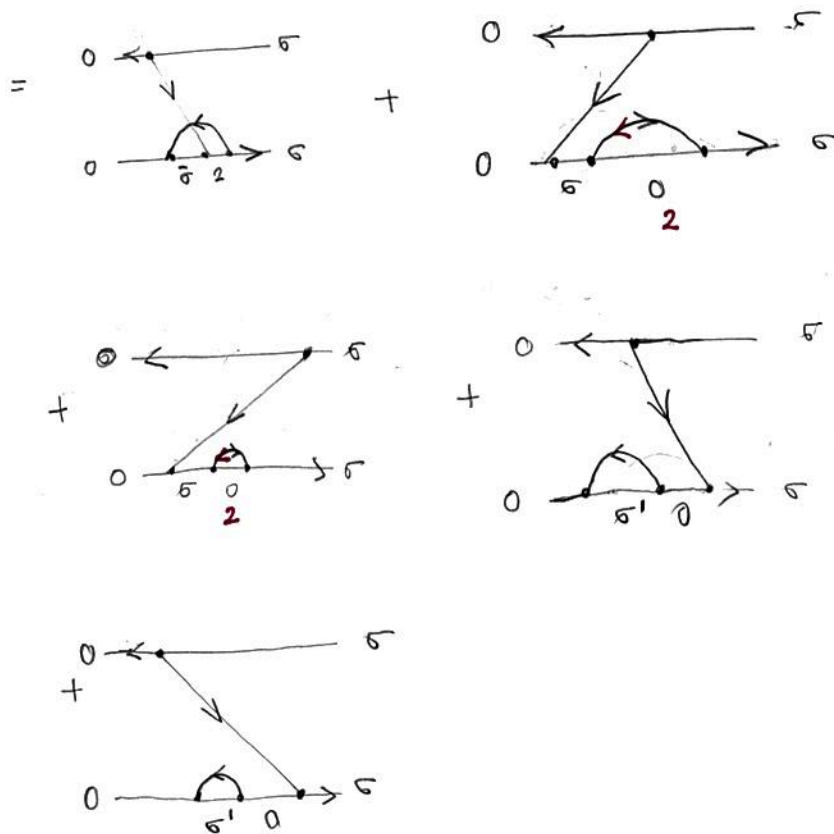
The diagrams $B_{(1|1)}$ should be included from the supergroup B .

However, for the AIM only $B_{(1|1)} \neq 0$ as $B_{(1|1)}$ is reducible.

For supergroups $B_{(1|1)}$ and $C_{(1|1)}$ the related diagrams describe a charge fluctuation in the initial, respectively final state.

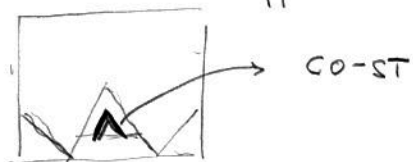
For example:

$$(K^{(4)})_{00}^{\sigma\sigma} = \Gamma^{\sigma \rightarrow 0} = (A_{(1|1)})_{00}^{\sigma\sigma} + (B_{(1|1)})_{00}^{\sigma\sigma} + (C_{(1|1)})_{00}^{\sigma\sigma}$$



In general co-st yields peaks inside the Coulomb diamond which, in contrast to the inelastic cot are gate dependent. It corresponds to transitions where the initial state is the excited state.

\Rightarrow these resonances forbidden in 2nd order appear above the inelastic cot tunneling threshold.



$(K^{(4)})_{00}^{00} : (A_{(2)})_{22}^{22}$ is excluded since $|2\rangle$ is an extremal state which does not accept further creation of particles. $B_{(0)}$ is excluded since it is a secular reducible diagram. On the other hand

$$(K^{(4)})_{22}^{\bar{5}\bar{5}} = \Gamma^{\bar{5}\bar{5}\rightarrow 2} = (A_{(4)})_{22}^{\bar{5}\bar{5}} + (B_{(2)})_{22}^{\bar{5}\bar{5}} + (C_{(2)})_{22}^{\bar{5}\bar{5}} \quad (4.77b)$$

where the $(B_{(2)})_{22}^{00}$ is excluded since $B_{(2)}$ cannot lead to a change in the particle number. The final step is the identification of the physical processes underlying each 4th order diagram.

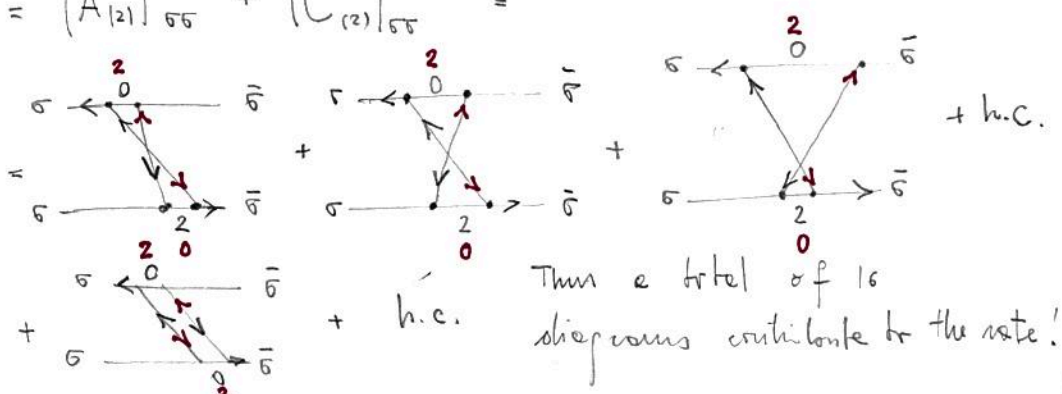
4.4.4 Fourth order processes

In this section we identify (or clarify) the fourth order processes from a more physical point of view: in this sense we denote by cotunnelling (cot), cotunnelling-assisted sequential tunnelling (co-st) and pair-tunnelling (pt) contributions where $\Delta N = 0$, $\Delta N = \pm 1$ and $\Delta N = \pm 2$, respectively.

■ Cotunnelling cot: $\Delta N = 0$

Examples of cotunnelling are the processes $\bar{5} \rightarrow \bar{5}$ or $|5\rangle \rightarrow |5\rangle$ or $|0\rangle \rightarrow |0\rangle$ or $|2\rangle \rightarrow |2\rangle$. Let us take for example, from (4.76c) the rate $\Gamma^{\bar{5}\bar{5}\rightarrow \bar{5}\bar{5}}$

$$\Gamma_{(4)}^{\bar{5}\bar{5}\rightarrow \bar{5}\bar{5}} = (K^{(4)})_{\bar{5}\bar{5}}^{\bar{5}\bar{5}} = (A_{(2)})_{\bar{5}\bar{5}}^{\bar{5}\bar{5}} + (C_{(2)})_{\bar{5}\bar{5}}^{\bar{5}\bar{5}} =$$



Notice that only 1 type of diagram from the C.121 group contributes to this cotunnelling rate since the others are reducible and secular (for the AIM).

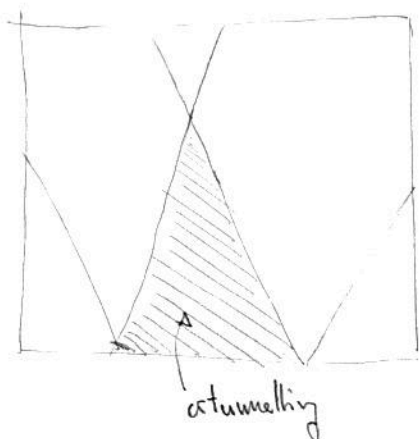
In general one distinguishes between elastic and inelastic cotunnelling:

i) ELASTIC cotunnelling: the initial and final states are the same or with the same energy \Rightarrow finite conductance background also in the Coulomb blockade region.

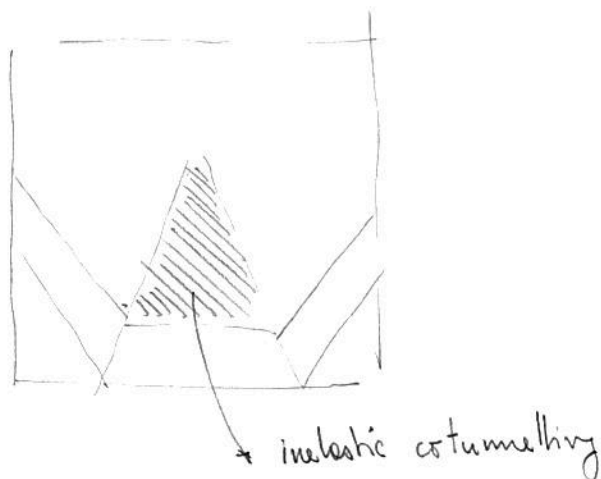
ii) INELASTIC cotunnelling: the initial and the final state do not have the same energy \Rightarrow this effect has a threshold in $V_b = E_f - E_i$.

Let us suppose that an external magnetic field is applied to the AIM yielding a Zeeman splitting $E_z = E_{\uparrow} - E_{\downarrow}$. The inelastic cotunnelling results in spectroscopy since at $V_b = E_z$ an additional line appears in the stability diagram. A coherent cotunnelling process can take one electron from source to drain leaving the dot in the excited state $|1\rangle$. This process involves the virtual occupation of the states $|0\rangle$ and $|2\rangle \Rightarrow$ it is algebraically suppressed by the energy of these states. Since the charge on the dot does NOT change, this process is independent of the gate voltage.

$$E_{\uparrow} = E_{\downarrow}$$

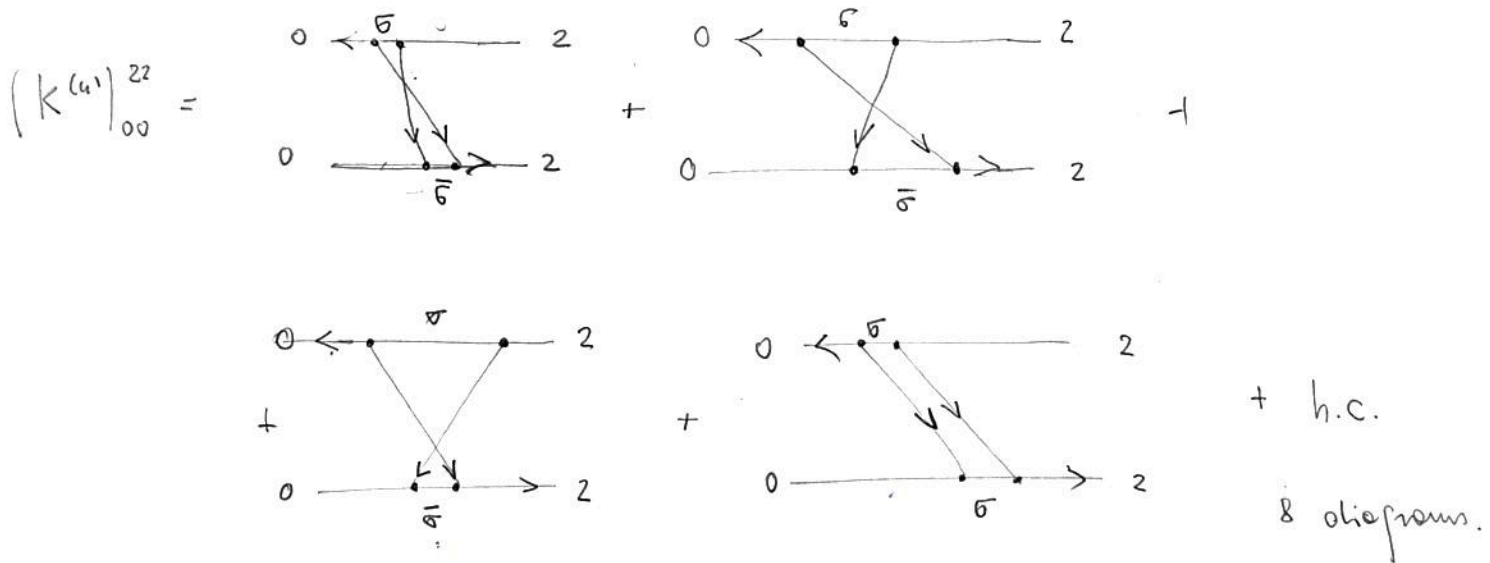


$$E_{\uparrow} \neq E_{\downarrow}$$

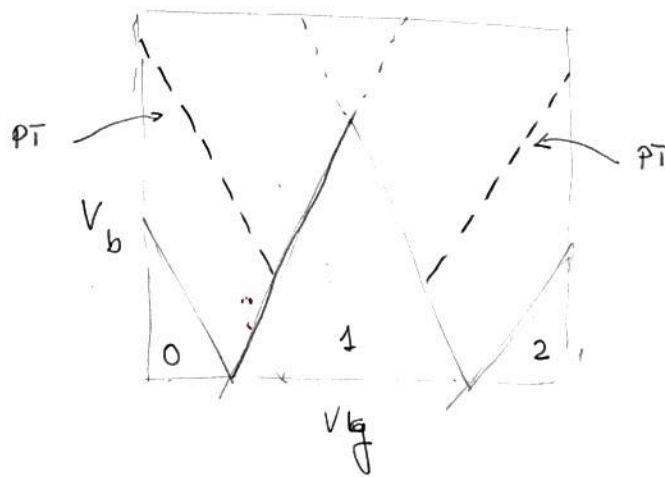


■ Pair-tunnelling (PT) In PT two electrons are coherently transferred between dot and leads. Let us pick up the process $|2\rangle \rightarrow |0\rangle$

$$(K^{(4)})_{00}^{22} = \Gamma^{2 \rightarrow 0} = (A_{(21)})_{00}^{22} + (C_{(21)})_{00}^{22}$$



Notice that the PT becomes energetically allowed at a lower bias than the sequential addition/removal $|0\rangle \rightarrow |1\rangle \rightarrow |2\rangle$ or $|2\rangle \rightarrow |1\rangle \rightarrow |0\rangle$.

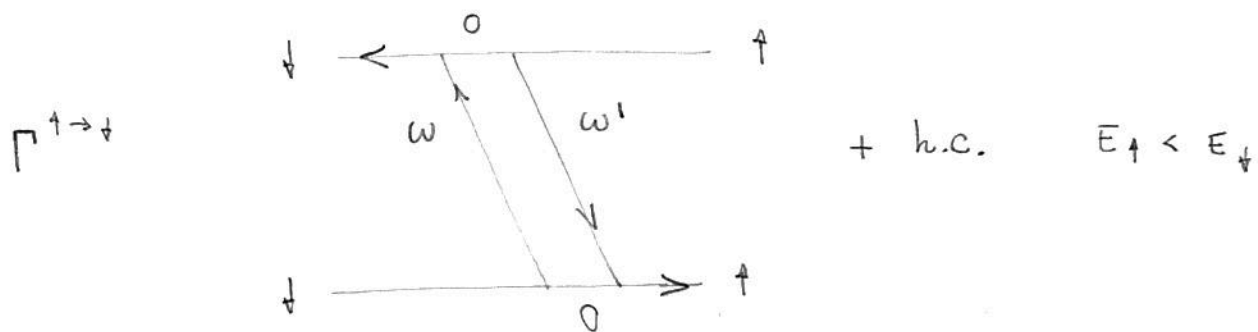


■ Cotunnelling-enabled seq. tunnelling (co-ST) and charge fluctuations

To identify the terms contributing to co-ST and charge fluctuations might be difficult, due to the gain-loss relationships. For example, the groups $A_{(21|1)}$ and $C_{(21|1)}$ provide merely the loss terms of the two electron transition processes. For the supergroups A and C

A case study: geometrical interpretation of the most relevant ^{component of the} cotunneling rate for AIM

Let us assume an AIM with magnetic field generating a Zeeman splitting



Following the diagrammatic rules one obtains for the diagram the following analytical expression

$$-\frac{i}{\hbar} \sum_{\alpha\alpha'} |T_{\alpha\alpha'}|^4 \int d\omega \int d\omega' \frac{f_{\alpha}^+(\omega) f_{\alpha'}^-(\omega')}{(E_0 - E_{\uparrow} + \omega' + i\eta)(E_{\uparrow} - E_{\uparrow} + \omega - \omega' + i\eta)(E_{\downarrow} - E_0 - \omega + i\eta)} + \text{c.c.} \quad (*)$$

We are interested mainly in the region in the bias and gate voltage in which the system is blocked (in the sequential tunnelling limit) into the ground state of one particle. This means:

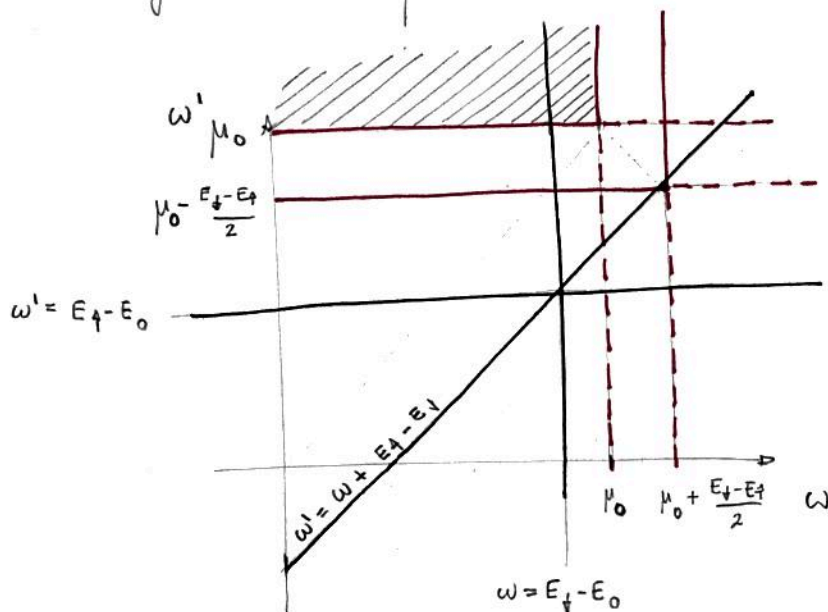
$$f_{\alpha}^+(E_{\uparrow} - E_0) \cong 1 \quad \alpha = L, R \quad \text{or, in other words}$$

$$E_{\uparrow} - E_0 \ll \mu_{\alpha}$$

In particular, to avoid also the interplay with the cotunneling-assisted sequential tunnelling, we restrict ourselves to the region

$$E_{\downarrow} - E_0 \ll \mu_{\alpha}$$

Now let's analyze the integrand in the ω, ω' space



- The black lines represent the zeros of the denominator.
- The red lines are the chemical potentials. The striped region is the relevant region when the product of the $f^+ f^-$ is ~ 4 .

If we do not relax the condition of being inside the Coulomb diamond there can be only 2 scenarios:

(A) * The shaded region includes only the vertical zeros $\omega = E_d - E_0$
 e.g. in equilibrium ($V_b = 0$) or if $\alpha = \alpha'$ or if $eV_b = \mu_L - \mu_R < E_d - E_f$

(B) * The shaded region includes the "vertical" zeros and the "tilted" zeros. $\alpha = L$ $\alpha' = R$ and $eV_b \geq E_d - E_f$.

The threshold $eV_b = E_d - E_f$ is clear if one imposes $\mu_{\alpha'} = \mu_{\alpha} + E_f - E_d$
 and $\alpha' = R \Rightarrow \mu_{\alpha'} = \mu_0 - \frac{eV_b}{2}$ and $\alpha = L \Rightarrow \mu_{\alpha} = \mu_0 + \frac{eV_b}{2}$

$$\cancel{\mu_0} - \frac{eV_b}{2} = \cancel{\mu_0} + \frac{eV_b}{2} + E_f - E_d \Rightarrow \boxed{eV_b = E_d - E_f}$$

[A] Due to the complex conjugation to be added to the rate one obtains 2Im of the double integral:

$$\begin{aligned} \text{Im}(z_1 z_2 z_3) &= (\text{Im} z_1) (\text{Re} z_2 \text{Re} z_3 - \text{Im} z_2 \text{Im} z_3) + \\ &+ (\text{Im} z_2) (\text{Re} z_1 \text{Re} z_3 - \text{Im} z_1 \text{Im} z_3) + \\ &+ (\text{Im} z_3) (\text{Re} z_1 \text{Re} z_2 - \text{Im} z_1 \text{Im} z_2) . \end{aligned}$$

In the limit $\eta \rightarrow 0$ the $\text{Im} \frac{1}{x+i\eta} = 0$ unless $x=0$. We conclude

$$\Gamma^{\uparrow \rightarrow \uparrow} \approx \sum_{\alpha\alpha'} \frac{2|\Gamma|''}{\hbar} \mathcal{D}_\alpha \mathcal{D}_{\alpha'} \int d\omega \int d\omega' \frac{f_\alpha^+(\omega) f_{\alpha'}^-(\omega')}{(E_0 - E_\uparrow + \omega')(E_\downarrow - E_\uparrow + \omega' - \omega)} \pi \delta(E_\downarrow - E_0 - \omega)$$

$$\approx \sum_{\alpha\alpha'} \frac{2|\Gamma|''}{\hbar} \mathcal{D}_\alpha \mathcal{D}_{\alpha'} \int_{\mu_{\alpha'}}^{\infty} d\omega' \frac{1}{(E_0 - E_\uparrow + \omega')(\cancel{E_\downarrow - E_\uparrow + \omega' - E_\downarrow + E_0})}$$

$$\approx \sum_{\alpha\alpha'} \frac{2\pi|\Gamma|''}{\hbar} \mathcal{D}_\alpha |\Gamma|'' \mathcal{D}_{\alpha'} \int_{\mu_{\alpha'}}^{\infty} d\omega' \frac{1}{(\omega' - E_\uparrow + E_0)^2} = \sum_{\alpha\alpha'} \Gamma_\alpha \frac{\hbar \Gamma_{\alpha'}}{2\pi(\mu_{\alpha'} - E_\uparrow + E_0)}$$

Inside the Coulomb diamond $\mu_{\alpha'} \gg E_\uparrow - E_0 \Rightarrow$ the scattering rate is small.

In particular $\sum_{\alpha\alpha'} \Gamma_\alpha \frac{\hbar \Gamma_{\alpha'}}{2\pi(\mu_{\alpha'} - E_\uparrow + E_0)} \ll \sum_{\alpha} \Gamma_\alpha \frac{\sum_{\alpha'} \hbar \Gamma_{\alpha'}}{k_B T}$.

[B] In this case the resonances to be taken into account are the one associated to the second and third denominator of (*).

$$\Gamma^{\uparrow \rightarrow \uparrow} \approx \Gamma_L \frac{\hbar \Gamma_R}{2\pi(\mu_R - E_\uparrow + E_0)} + \Gamma_L \frac{\hbar}{2\pi} \Gamma_R \int d\omega \int d\omega' \frac{f_L^+(\omega) f_R^-(\omega')}{(E_0 - E_\uparrow + \omega')(E_\downarrow - E_0 - \omega)} \delta(E_\downarrow - E_\uparrow + \omega' - \omega)$$

$$\begin{aligned} x &= \frac{\omega + \omega'}{2} \\ y &= \omega' - \omega \end{aligned} = \frac{\Gamma_L \Gamma_R \hbar}{2\pi} \left(\frac{1}{\mu_0 - \frac{eV_b}{2} - E_\uparrow + E_0} + \int dx \int dy \frac{f_L^+(x - \frac{y}{2}) f_R^-(x + \frac{y}{2})}{(E_0 - E_\uparrow + x + \frac{y}{2})(E_\downarrow - E_0 - x + \frac{y}{2})} \delta(E_\downarrow - E_\uparrow + y) \right)$$

$$\Gamma_{\uparrow \rightarrow \downarrow} = \frac{\Gamma_L \Gamma_R \hbar}{2\pi} \left(\frac{1}{\mu_0 - \frac{eV_b}{2} - E_{\uparrow} + E_0} + \Theta(SV_b) \int_{\mu_0 - \frac{SV_b}{2}}^{\mu_0 + \frac{SV_b}{2}} dx \frac{1}{(E_0 - E_{\uparrow} + \frac{E_{\uparrow} - E_{\downarrow}}{2} + x)} \frac{1}{(E_{\downarrow} - E_0 + \frac{E_{\uparrow} - E_{\downarrow}}{2} - x)} \right)$$

$$SV_b = eV_b - (E_{\downarrow} - E_{\uparrow})$$

$$\mu_R = \mu_0 - \frac{eV_b}{2} \quad \tilde{\mu}_R = \mu_R - E_{\uparrow} + E_{\downarrow} = \mu_0 - \frac{eV_b}{2} - E_{\uparrow} + E_{\downarrow}$$

$$x = \frac{\tilde{\mu}_R + \mu_R}{2} = \mu_0 - \frac{eV_b}{2} - \frac{E_{\uparrow} - E_{\downarrow}}{2} = \mu_0 - \frac{SV_b}{2}$$

$$\mu_L = \mu_0 + \frac{eV_b}{2} \quad \tilde{\mu}_L = \mu_L + E_{\uparrow} - E_{\downarrow} = \mu_0 + \frac{eV_b}{2} + E_{\uparrow} - E_{\downarrow}$$

$$x = \frac{\mu_L + \tilde{\mu}_L}{2} = \mu_0 + \frac{SV_b}{2}$$

$$= \frac{\Gamma_L \Gamma_R \hbar}{2\pi} \left(\frac{1}{\mu_0 - \frac{eV_b}{2} - E_{\uparrow} + E_0} - \Theta(SV_b) \int_{\mu_0 - \frac{SV_b}{2}}^{\mu_0 + \frac{SV_b}{2}} dx \frac{1}{\left(x + E_0 - \frac{E_{\uparrow} + E_{\downarrow}}{2}\right)^2} \right)$$

$$= \frac{\Gamma_L \Gamma_R \hbar}{2\pi} \left(\frac{1}{\mu_0 - \frac{eV_b}{2} - E_{\uparrow} + E_0} + \Theta(SV_b) \left[\frac{1}{\left(\mu_0 + \frac{SV_b}{2} + E_0 - \frac{E_{\uparrow} + E_{\downarrow}}{2}\right)} - \frac{1}{\mu_0 - \frac{SV_b}{2} + E_0 - \frac{E_{\uparrow} + E_{\downarrow}}{2}} \right] \right)$$

$$= \frac{\Gamma_L \Gamma_R \hbar}{2\pi} \left(\frac{1}{\mu_0 - \frac{eV_b}{2} - E_{\uparrow} + E_0} + \Theta(eV_b - (E_{\downarrow} - E_{\uparrow})) \left(\frac{1}{\mu_0 + \frac{eV_b}{2} - E_{\downarrow} + E_0} - \frac{1}{\mu_0 - \frac{eV_b}{2} - E_{\uparrow} + E_0} \right) \right)$$

More precisely one should put together all contributions:

- $\alpha = \alpha'$ we have, independently from the applied bias, the contribution to the transition rate

$$\sum_{\alpha} \frac{\hbar \Gamma_{\alpha}^2}{2\pi (\mu_{\alpha} - E_{\uparrow} + E_0)} = \frac{\hbar \Gamma_L^2}{2\pi} \left(\frac{1}{\mu_0 + \frac{eV_b}{2} - E_{\uparrow} + E_0} + \frac{1}{\mu_0 - \frac{eV_b}{2} - E_{\uparrow} + E_0} \right)$$

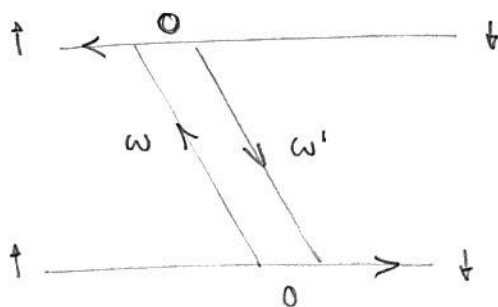
- $\alpha = L \quad \alpha' = R$

$$\frac{\hbar}{2\pi} \Gamma_L \Gamma_R \left(\frac{1}{\mu_0 - \frac{eV_b}{2} - E_{\uparrow} + E_0} + \Theta(eV_b - (E_{\downarrow} - E_{\uparrow})) \left(\frac{1}{\mu_0 + \frac{eV_b}{2} - E_{\downarrow} + E_0} - \frac{1}{\mu_0 - \frac{eV_b}{2} - E_{\downarrow} + E_0} \right) \right)$$

- $\alpha = R \quad \alpha' = L$

$$\frac{\hbar}{2\pi} \Gamma_L \Gamma_R \Theta(\mu_0 - \frac{eV_b}{2} - E_{\downarrow} + E_0) \frac{1}{\mu_0 + \frac{eV_b}{2} - E_{\uparrow} + E_0}$$

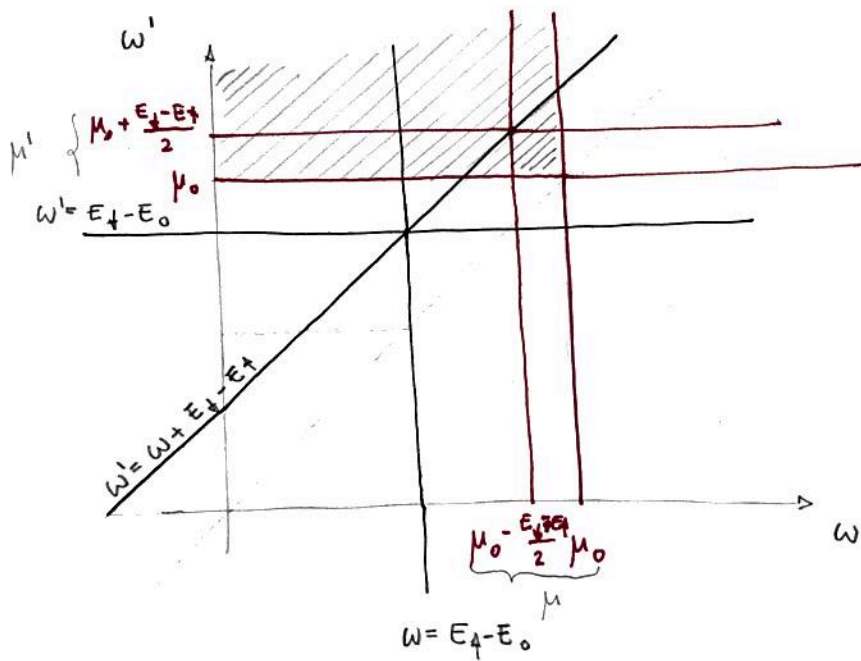
In order to complete the picture one needs to calculate also:



The role of the spins is now completely reversed

$$\Gamma_{\downarrow \rightarrow \uparrow} \approx -\frac{i}{\hbar} \sum_{\alpha \alpha'} |z|^4 \mathcal{D}_{\alpha} \mathcal{D}_{\alpha'} \int d\omega \int d\omega' \frac{f_{\alpha}^+(\omega) f_{\alpha'}^-(\omega')}{(E_0 - E_{\downarrow} + \omega' + i\eta)(E_{\uparrow} - E_{\downarrow} + \omega' - \omega + i\eta)(E_{\uparrow} - E_0 - \omega + i\eta)}$$

The associated resonance/chemical potentials scheme now is



All contributions to the rate $\Gamma^{\downarrow \rightarrow \uparrow}$ read

- $\alpha = \alpha'$ Both the vertical and the tilted resonance lines contribute to the rate

$$\begin{aligned}
 & \sum_{\alpha} \frac{\Gamma_{\alpha}^2 \hbar}{2\pi} \left(\int_{-\infty}^{\infty} d\omega' \frac{1}{\mu_{\alpha} (E_0 - E_{\downarrow} + \omega') (E_{\uparrow} - E_{\downarrow} + \omega' - E_{\uparrow} + E_0)} \right) + \int_{-\infty}^{\infty} dx \frac{1}{\mu_0 + \frac{E_{\downarrow} - E_{\uparrow}}{2} (E_0 - E_{\downarrow} + x + \frac{E_{\downarrow} - E_{\uparrow}}{2}) (E_{\uparrow} - E_0 - x + \frac{E_{\downarrow} - E_{\uparrow}}{2})} \\
 &= \sum_{\alpha} \frac{\Gamma_{\alpha}^2 \hbar}{2\pi} \left(\frac{1}{E_0 - E_{\downarrow} + \mu_{\alpha}} \right) + \sum_{\alpha} \frac{\Gamma_{\alpha}^2 \hbar}{2\pi} \int_{-\infty}^{\infty} dx \frac{-1}{\mu_{\alpha} + \frac{E_{\downarrow} - E_{\uparrow}}{2} (E_0 - \frac{E_{\downarrow} + E_{\uparrow}}{2} + x)^2} \\
 &= \sum_{\alpha} \frac{\Gamma_{\alpha}^2 \hbar}{2\pi} \left(\frac{1}{E_0 - E_{\downarrow} + \mu_{\alpha}} \right) + \sum_{\alpha} \frac{\Gamma_{\alpha}^2 \hbar}{2\pi} \left(\frac{1}{\mu_{\alpha} + E_0 - E_{\uparrow}} - \frac{1}{\mu_{\alpha} + E_0 - E_{\downarrow}} \right) \\
 &= \sum_{\alpha} \frac{\Gamma_{\alpha}^2 \hbar}{2\pi} \frac{1}{\mu_{\alpha} + E_0 - E_{\uparrow}} \quad \left(\text{N.B. this formula does not take into account the situation in which the triple point enters the integration region!} \right)
 \end{aligned}$$